IEEE *Access*
Multidisciplinary : Rapid Review : Open Access Journal

Energy Saving and Reliability for Wireless Body Sensor Networks (WBSN)

Hisham Alshaheen[1, 2], and Haifa Takruri Rizk[1]
[1]School of Computing, Science & Engineering, University of Salford, Great Manchester, United Kingdom
[2]College of Science, University of Thi- Qar, Iraq

Corresponding author: Hisham Alshaheen (e-mail: h.s.s.alshaheen@edu.ac.uk).

ABSTRACT In healthcare and medical applications, the energy consumption of biosensor nodes affects the collection of biomedical data packets, which are sensed and measured from the human body and then transmitted toward the sink node. Nodes that are near to the sink node consume more energy as all biomedical packets are aggregated through these nodes when communicated to sink node. Each biosensor node in a wireless body sensor networks (WBSNs) such as ECG (Electrocardiogram), should provide accurate biomedical data due to the paramount importance of patient information. We propose a technique to minimise energy consumed by biosensor nodes in the bottleneck zone for WBSNs, which applies the Coordinated Duty Cycle Algorithm (CDCA) to all nodes in the bottleneck zone. Superframe order (SO) selection in CDCA is based on real traffic and the priority of the nodes in the WBSN. Furthermore, we use a special case of network coding, called Random Linear Network coding (RLNC), to encode the biomedical packets to improve reliability through calculating the probability of successful reception (PSR) at the sink node. It can be concluded that CDCA outperforms other algorithms in terms of energy saving as it achieves energy savings for most biosensor nodes in WBSNs. RLNC employs relay nodes to achieve the required level of reliability in WBSNs and to guarantee that the biomedical data is delivered correctly to the sink node.

INDEX TERMS Duty Cycle (DC), Energy Consumption, Network Coding (NC), Wireless Body Sensor Network (WBSN), Reliability

I. INTRODUCTION

A Wireless Body Sensor Network (WBSN) consists of several biological sensors and represents a special case of a Wireless Sensor Network (WSN). WBSNs are used in both medical and non-medical applications to monitor human body conditions[1]. Figure 1 shows an example of WBSN topology with implantable medical devices and the wearable medical devices [2].

In WBSN applications, the measurement of multiple medical parameters is required to observe patients in a hospital using biomedical sensor nodes which are implanted inside the body of the patient or attached to the patient. Examples include ECG, temperature, oxygen saturation, heart rate, and blood pressure. Also, the monitored patient requires more attention because emergency or abnormal medical data is pertinent to the life of the patient. Therefore, the energy usage of each biosensor node and the reliable data transmission is of immense significance in WBSNs. WBSN parameters such as the distances and locations of the biomedical sensor nodes on the human body relative to the sink node, WBSN topology which includes the adding of the relay node, and the propagation model, for instance line of sight (LOS) and non-line of sight (NLOS) propagation, affect reliable energy saving for WBSNs.

This paper contributes a novel Coordinated Duty Cycle Algorithm (CDCA) and describes the mechanisms of its implementation. For instance, calculation of the slots
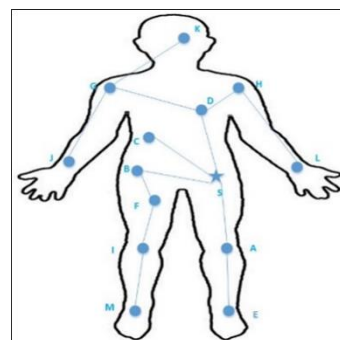

Figure 1. WBSN topology with 13 biosensors

1

algorithm; identification of priority with the equations used to determine the queue state value; selection of the type of slots, such as CAP (Contention Access Period) slots and GTS (Guaranteed Time Slots) slots; and effects of the number of remaining pending packets in the queue and received packets at the sink node. The CDCA is implemented in the WBSN model, which uses RLNC. This paper also includes analysis of the results and reports on the significant reduction in energy consumption for the nodes in WBSNs and the achieved level of reliability whereby the biomedical data would be delivered correctly to the sink node.

The paper is organised as follows. Section II reviews the RLNC technique. Section III describes the related work. Section IV shows the model design of the Body Area Network (BAN). Section V presents the proposed design for the CDCA approach. Section VI describes the reliability of the proposed WBSN model design. Section VII presents the simulation. The conclusions are drawn in Section VIII. Finally, Section IX presents Appendix A that provides information about some laws of probability theorem and analysis of the proposed scheme.

II. RLNC technique

The term 'network coding' (NC) was used for the first time by Ahlwede in 2000 in an article entitled Network Information Flow[3]. A random linear network coding (RLNC) approach is defined by [4] and [5]. In the RLNC approach, the nodes transmit the linear combination of the incoming packets to the outgoing edges, utilising randomly and independently chosen coefficients of code from some finite fields. However, on the receiver side, a decoder is needed to compute the overall linear combinations of source processes. The authors computed a lower bound on coding success probability in networks with unreliable links, amount of redundancy, and in terms of link failure probability[5].

The Encoding procedure: to compute the encoding of the packets, the node chooses a sequence coefficient $q = (q_1, q_2, q_3, ..., q_n)$ from Galois Field $GF(2^s)$, which is called an encoding vector. The single output encoded packet is calculated as the sum of products of each of the n native packets that are received at a node $G_i (i = 1, 2, 3, ..., n)$ with a random coefficient q_i. The output encoded packet is described below.

$$Y = \sum_{i=1}^{n} q_i G_i \qquad q_i \in GF(2^s) \qquad (1)$$

Where Y and G_i are the coded and original packets, respectively, the encoded packets with the coefficients are transmitted to the destination node. The receiver side uses the encoding vector to decode the encoded packets.

Decoding procedure: The network coded data with the encoding vector q are received at the destination. Supposing the node has received a set of packets $(q^1, Y^1), ... (q^m, Y^m)$,

the symbols Y^j and q_i^j represent the jth received packet for the encoded packet and coding vector respectively.

$$Y^j = \sum_{i=1}^{n} q_i^j G_i \qquad j = 1, ..., m \qquad (2)$$

Where Y^j and q_i^j represent the network coded data and encoding vector respectively, the recipients must receive at least n linearly independent packets to decode the original packets. In the above equation (2), the term G_i is unknown, which comprises the native packets transmitted in the network. By using the linear system in equation (2), the receiver side can retrieve the number of native packets. We can recover all source packets by Gaussian elimination, if global encoding vector is full rank [6].

III. Related work

The concept of switching the node to active or sleep mode can be achieved with a duty cycle. The nodes can be activated whenever they need to transmit the data to the sink node; otherwise they will be in sleep mode to reduce the energy consumption [7]. In [8], the authors propose a novel DC adaptation (DCA) algorithm for the beacon-enabled approach based on IEEE 802.15.4. The DCA algorithm achieves increased energy efficiency and serves to minimise the packet drop when it employs the duty cycle. However, DCA uses a fixed beacon interval (BI) which could increase energy consumption if the value of the beacon order (BO) is smaller [8].

In an IEEE 802.15.4-based WSN (wireless sensor network), the researchers propose a Dynamic Duty Cycle Adaptation to Real time data (DDCAR); the proposed algorithm adapts the duty cycle in order to minimise the packet delay and improve time of delivery of the real time data; the coordinator node immediately extends the active period to adjust the period of real time traffic through the switching time between a node and a coordinator node[9]. In addition, an Individual Beacon Order Adaptation (IBOA) Algorithm is proposed for IEEE 802.15.4. The IBOA algorithm considers reducing the energy consumption; it uses individual beacon order adaption and DC at the same time[10]. Gadallah and Jaafari in [11] have introduced a reliable energy-efficient WSNs MAC scheme which is dependent on IEEE 802.15.4 non-beacon enabled mode. The experimental results of the proposed mechanism generally performed better than the standard protocol (IEEE 802.15.4) in terms of parameters such as energy conservation and all traffic types.

In [12], the authors proposed a DCLA (Duty Cycle Learning Algorithm) which adapts the duty cycle in order to decrease the energy usage. Although the energy consumption is reduced, DCLA could not be implemented by the testbed or simulations because it involves more complicated calculation. The DCLA is considered only for fixed traffic[12]. Moreover, in [13], the researchers present AAOD (Adaptive Algorithm to Optimize the Dynamics) for IEEE 802.15.4 networks to reduce energy consumption.

Although the AAOD algorithm can reduce the number of collisions and it is compliant with IEEE 802.15.4, the consumed energy is higher than other algorithms and AAOD does not consider traffic deadlines and congestion level. Also, in [14], the researchers have examined the impact of changing values of BO and SO on medium access delay, energy consumption, and packet loss ratio. In the simulation scenario, the authors used two biosensor nodes (ECG and blood analysis module) in order to study the MAC protocol parameter for the network behaviour and also for reducing energy consumption.

In [15], the researchers propose a dynamic and self-adaptive algorithm, used to adjust a DC based on the adjustment of beacon order (BO) and superframe order (SO), which is termed DBSAA (Dynamic Beacon Interval and Superframe Adaptation Algorithm). However, DBSAA supposes that all nodes in the networks use the same data rate. Furthermore, In [16], the researchers propose a new Adaptive Duty Cycle Algorithm (ADCA) to improve energy efficiency based on beacon-enabled WSN. The coordinator node collects network information, such as the queue state of the nodes and the idle time; it enhances the capability for estimation of the network traffic, and it adjusts the DC of the network. The ADCA increases the accuracy and the speed of adjustment for the duty cycle. In [17], the authors propose a novel mathematical model for body area network (BAN) topology. This model uses the coordinated duty cycle (CDC) technique and Random Linear Network Coding (RLNC) to improve energy efficiency in the bottleneck zone, however, the authors used binary tree to implement it.

Researchers have used the cooperative coding scheme, which integrates cooperative communication and network coding [18]. The network coding could improve communication reliability and reduce the number of packet transmissions. Furthermore, the proposed scheme achieves a significant improvement in the reliability and throughput with analysis of the probability of successful reception at the destination node [18]. Another study proposed Network Coding-based Cooperative Communications scheme (NCCC) at the source cluster where the NCCC encodes original packets with random network coding [19]. In this study, the authors also consider packet delivery reliability in multi hop relay WSNs [19].

In [20], the authors used cooperation network coding (CNC) to improve the reliability of WBSNs in the case of node failure or links failure. However, the proposal was not adaptive to dynamic network conditions because the nodes were fixed. Moreover, a number of researchers have presented and contrasted the novel approaches of Cooperative Network Coding (CNC) and Cooperative Diversity Coding (CDC) to increase the reliability and enhance the throughput of the wireless body area networks (WBAN). With respect to the proposed approaches, CDC reveals higher throughput than CNC because the biomedical packets and coded packets are transmitted to the destination node while in CNC only the

coded packets are transmitted to the destination node. Then, to decode the original packets, the destination node should receive a number of coded biomedical packets that are at least equal to the number of the original packets[21]. Cooperative Diversity Coding (CDC) is used to code the biomedical packets. In addition, the proposed scheme achieves the level of performance of CNC and CDC in terms of the probability of successful reception at the destination node as well as the required level of reliability in WBSNs [22].

With regard to RLNC, researchers have proposed a novel cooperative transmission scheme based on demodulate-and-forward and network coding for WBSNs [23]. The study proposed Random XOR Network Coding (RXNC) to improve the reliability of WBSNs, and the source node transmits to the relay node, which demodulates the received packet. After this, each relay selects different coded symbols from demodulated symbols and XORs them to create the network coded symbol. Moreover, the authors calculated the error probability of the created network coded symbols and computed the optimum value to minimise the error probability [23].

However, the energy consumption of nodes is still a problem and a challenge in WBSNs, especially for the biosensor nodes placed next to the sink node; these nodes consume more energy because all biomedical packets are aggregated through these nodes forming a bottleneck zone. Furthermore, in [24], there is energy wastage in the bottleneck zone because the nodes are placed near the sink node, which causes them to consume more energy and deplete energy quickly. Consequently, this area has heavy traffic which limits the network lifetime[24]. Also, the reliable transmission of physiological data is still a challenge for WBSN and medical monitoring systems, and this needs to be considered and developed[25][26].Recently, there have been studies published on the combination of duty cycle (DC) and network coding (NC). In [27], Rout and Ghosh combined the random duty cycle with NC to enhance the network lifetime in WSN; they applied XOR NC only to the NC node in the bottleneck zone. However, simple nodes have no benefit from NC in terms of reducing energy usage and the reliability of data delivery is reduced by XOR NC. Lee et al [28] proposed a technique using a random duty cycle with RLNC in the bottleneck area to improve energy efficiency and reliability. The sensor nodes near the sink deplete their energy due to heavy traffic, which limits the network lifetime[28].

Although previous work considered adjusting duty cycle for sensor nodes which implement the IEEE 802.15.4 MAC standard, the majority of the previous studies did not review the energy consumption of biosensor nodes in the bottleneck for WBSNs based on priority and traffic changes, and likewise for most work which uses random duty cycle. The main problems in the bottleneck zone are energy wastage and lost biomedical packets in this area. To address the problems a combination between the coordinate duty cycle algorithm

(CDCA) and the random linear network coding (RLNC) is proposed.

IV. The model of wireless body sensor network

With regard to the system model in Figure 2, the researchers propose a novel mathematical model for body area network (BAN) topology to explain the deployment and connection between biosensor nodes, simple relay nodes, NC relay nodes and the sink node. Moreover, the proposed approach uses Duty Cycle (DC) and RLNC to improve the energy efficiency for the nodes in the bottleneck zone [17].

In this paper, the design of coordinated duty cycle algorithm (CDCA) is proposed to a correctly select a SO based on the real behaviour of traffic and the priority of the sensor nodes. The combination of the CDCA approach and RLNC type is applied to enhance the energy efficiency and improve the reliability in the bottleneck zone.

In this paper, a general case WBSN topology is illustrated in Figure 3, including 13 biosensor nodes, which are placed on the human body. The biosensors comprise EMG sensor (nodes A and I), body temperature sensor (node B), ECG sensor (node D), glucose monitor sensor (node F), and blood pressure monitor (node H). The distance between the biosensor nodes and sink node for the single-hop technique and the multi-hop technique is shown in Table I.

In the WBSN model, simple relay nodes and NC relay nodes are added to the WBSN topology, as shown in Figure 4(right–hand side). Node B and node C are connected directly to the sink given the short distance between them at 0.3m and 0.2m respectively. The extended WBSN topology is illustrated on the right-hand side and a sample topology is shown on the left hand side, which includes a biomedical sensor node (A), a simple relay node (R), a NC relay node (NC), and the sink node (S).

V. The proposed design for CDCA approach

The selection of the superframe order (SO), which represents the summation for the number of GTS (Guaranteed Time Slots) slots and the number of CAP (Contention Access Period) slots, plays the main role in the energy consumption and successful delivery of the biomedical data in WBSN, which has an impact on the performance of the WBSN, for instance, if the value of SO is high and the traffic is low or there is no traffic. The setting of SO for a long period is not necessary, and it causes an increase in the energy consumption and a delay. In addition, when the value of SO is small, and traffic is high, the network will not be able to process all biomedical packets, which causes the loss of a number of packets. In this situation, the biosensor nodes will save energy but most biomedical packets will be dropped. Hence, the correct selection of the SO based on information about the real traffic and the priority of the nodes in WBSN results in energy saving and delivery of the biomedical packets to the sink node. .
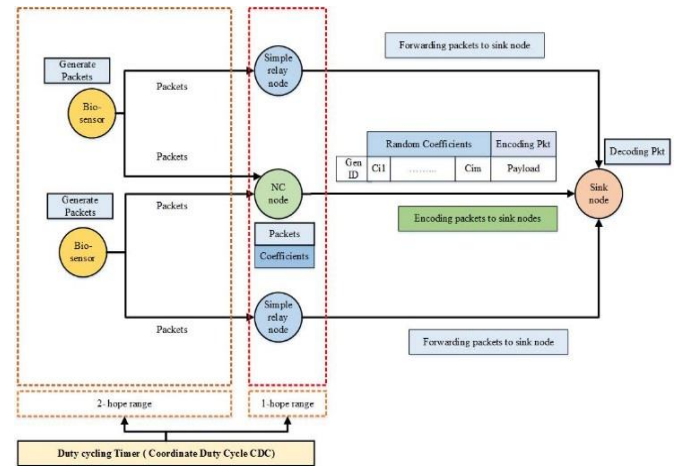

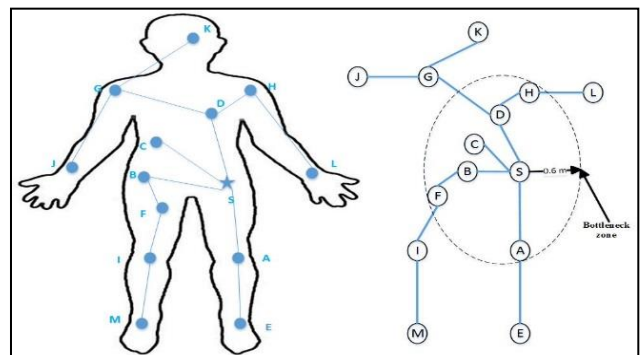Figure 2. The model of the WBSN which employs duty cycle

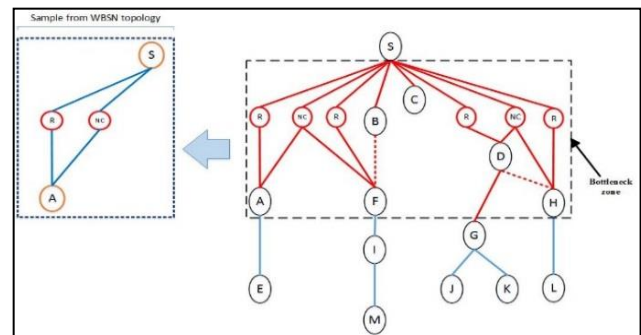Figure 3. Human body with 13 biomedical sensor nodes and the WBSN topology

Figure 4. Tree topology for WBSN with one sample from WBSN topology

TABLE I
THE DISTANCE (METERS) BETWEEN BIOSENSOR NODE AND SINK NODE FOR THE SINGLE HOP, AND BETWEEN THE BIOSENSOR AND THE NEAREST NODE FOR THE MULTI-HOP

Sensor	A	B	C	D	E	F	G
Single -Hop	0.6	0.3	0.2	0.5	1.2	0.6	0.7
Multi -Hop	0.6	0.3	0.2	0.5	0.6	0.3	0.2
Sensor	H	I	J	K	L	M	
Single -Hop	0.6	0.8	1.0	0.8	0.8	1.5	
Multi -Hop	0.1	0.3	0.6	0.4	0.6	0.6	

With respect to [29],[30],[31], there are different kinds of data, for instance, critical data (CD), normal data (ND), delay sensitive data (DSD) and reliability sensitive data (RSD), which generate from the nature of WBSNs. In this paper, the biosensor node generated data is classified into two types: normal data and critical data. We explain the steps of CDCA as follows:

A. The calculation for the initial slots in WBSN

In WBSN, the data rate is heterogeneous for the biosensor nodes, for example, ECG (Electrocardiography), EEG (Electroencephalography), EMG (Electromyography), blood pressure, and the body temperature sensor, which have 192 Kbps, 86.4 Kbps, 1536 Kbps, 1.92 Kbps, and 1 Kbps, respectively. The number of slots for nodes in WBSN is calculated depending on the data rate and the slots represent the initial values, which are used by the sink node in the study's algorithm. Figure 5 shows the procedure for the calculation of the slots in WBSN.

Table II shows the results obtained from the calculation of the slots for nodes in WBSN. The results are kept in the sink node as an array, which represents the initial value in the researcher's algorithm. The sink node has initial slots for each of them such as four slots for ECG, two slots for EEG, and one slot for the blood pressure for the transmission of the biomedical data. Moreover, the medical staff could identify the priority for the nodes in WBSN based on the patient case. Then, the sink node allocates the slots to the node as a Guaranteed Time Slots (GTS) if the node has high priority, and allocates the slots as the Contention Access Period (CAP) if the node has a low priority.

B. The development in the reserved field

Essentially, in the proposed algorithm, the sink node has an array, which includes all information about the biosensor nodes in WBSN such as data rate, the position of the node, and the queue state. The sink node calculates the SO for each biosensor node based on the data rate, which represents the initial values, and saves and updates the value of the SO for each node in the array. Therefore, the configuration of the SO by the sink node indicates the default setting and represents a start point in the proposed algorithm. Then, the SO is adjusted proportionally based on the real behaviour of traffic over time for biomedical data, which is generated through sensing or measuring the vital signs of the human body.

With respect to the standard IEEE 802.15.4, the reserved field in the standard MAC header contains three bits (7-9 bits in the frame control field). Moreover, the bits of the reserved field are set to zero on the transmission and are ignored on the reception. However, in the proposed algorithm, three bits of the reserved field are used as follows: One bit is used to present the level of priority and two bits are used to present the queue state for each node in WBSN.
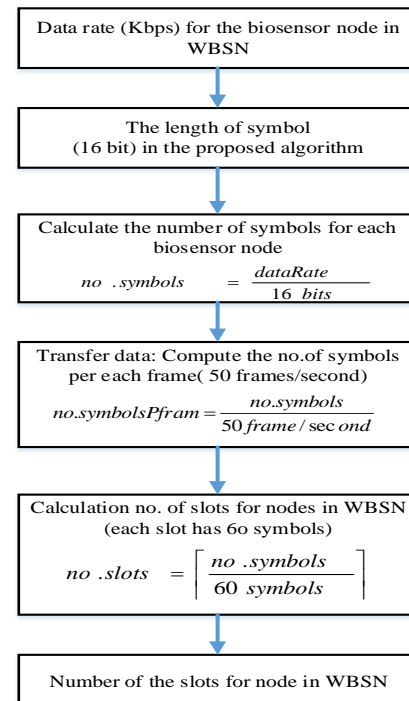

Figure 5. The procedure for the calculation of the slots in WBSN, which represent the initial value for the nodes

TABLE II

THE PROCEDURE OF THE CALCULATION THE NUMBER OF SLOTS FOR THE BIOSENSOR NODES IN WBSN

Bio-sensor node	Data rate (Kbps)	Symbol Size (bit)	No. of symbol per sec. (Ksymbols /sec)	No. symbol per frame (symbols)	No. slots
ECG	192	16	12	240	4
EEG	86.4	16	5.4	108	2
EMG	1536	16	96	1920	32
Blood pressure	1.92	16	0.12	2.4	1
Body temperature	1	16	0.0625	1.25	1
Pulse rate	2.4	16	0.15	3	1
Motion sensor	35	16	2.1875	43.75	1
Blood saturation	16	16	1	20	1

Furthermore, the queue state is equal to zero when the node has no pending packet, and in another case there are three levels for the queue state. In addition, the sink node updates the array for all biosensor nodes in WBSN.

Firstly, one bit is allocated to the priority level. The medical staff might identify the priority of the biosensor nodes depending on the case of the patient. The sink node allocates GTS in the Contention Free Period (CFP) to the biosensor nodes, which have high priority. The priority of the biosensor node is represented by one bit, and the high priority is equal to one, which presents the critical data, whereas the low priority is equal to zero, which presents normal data, as shown in Figure 6 for low priority, the sink node allocates CAP slots for the biosensor nodes in WBSN.
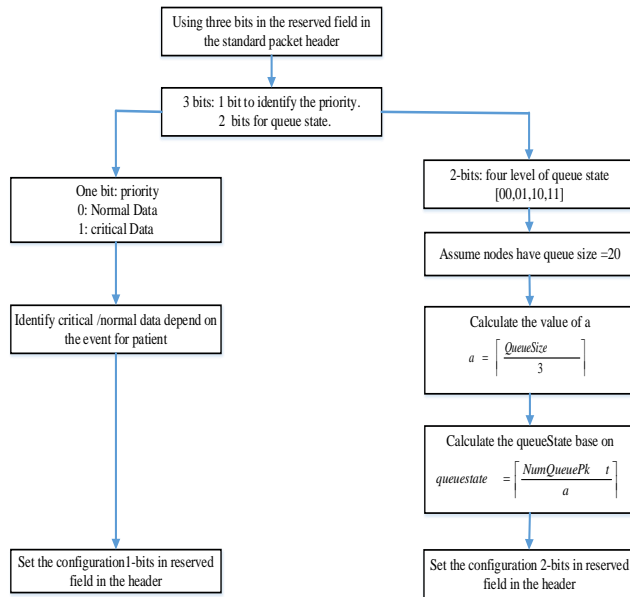
Figure 6. The three bits of the reserved field

Figure 7. The algorithms for the priority of the biosensor node in WBSN

Secondly, the next two bits are used to show the queue state for the biosensor node in WBSN. The sink node receives information from the biosensor node about the queue state, which helps to estimate the network traffic. The queue state can be calculated as shown in equation (3) and (4). Where NumQueuePkt is the number of biomedical packets inside the queue and QueueSize represents the maximum number of biomedical packets, which can be kept in the queue of the node.

$$queueState = \left\lceil \frac{NumQueuePkt}{a} \right\rceil \tag{3}$$

$$where \qquad a = \left\lceil \frac{QueueSize}{3} \right\rceil \tag{4}$$

C. Coordinated Duty Cycle Algorithm (CDCA)

As far as the priority is concerned, when the patient is at risk and it is a critical case, medical staff should choose the biosensor nodes such as heart rate or electrocardiograms, and they give the priority to the nodes depending on the patient case. Therefore, the generation of the biomedical packets from nodes represent critical data (CD) for the patient. The critical data has a high priority in the algorithm of the priority, as shown in Figure 7, and needs a certain amount of time for transmission and the highest reliability in WBSN. Furthermore, the sink node allocates the slots, which are termed GTS in the CFP depending on the algorithm of SO as presented in Figure 8. Then, the sink node updates the format of GTS fields for the node in the MAC header. The sink node checks the current GTS slots with the maximum value of the BO in the system. Moreover, it accurately allocates the GTS slots for biomedical nodes in order to save energy consumption and ensures successful delivery of biomedical packets.

The sink node allocates the GTS for the nodes which have a high priority and allocates the remaining slots to the nodes
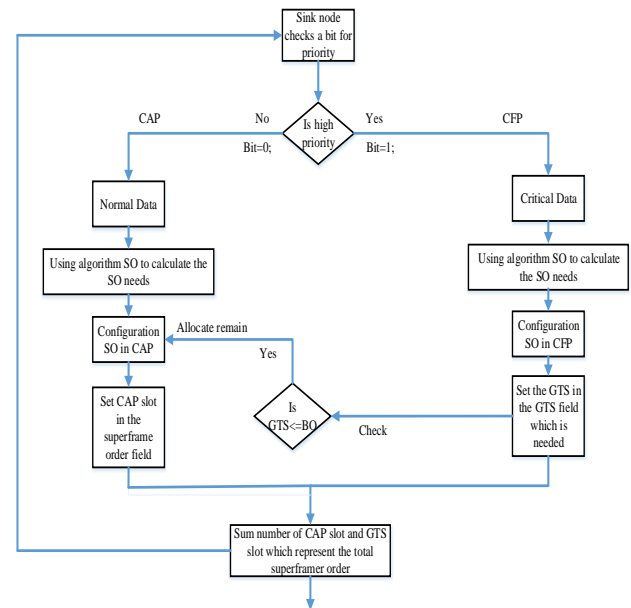
with low priority, as presented in Figure 7, and the slot is termed the CAP.

The CDCA algorithm calculates the number of slots for each biosensor node according to the ratio between the remained numbers of pending packets at the queue for the biosensor node to the received number of packets at the sink node. The initial value of slots was calculated for the biosensor nodes in WBSN, as previously reported by the researchers' algorithm. Moreover, the value of Beacon order (BO) should define the CDCA algorithm. Therefore, the total value of the SO should not exceed the maximum of the BO, as shown in Figure 7. The proposed algorithm computes the value of the SO for the nodes depending on the real behaviour of the traffic in the WBSN. In CDCA, the sink node compares between the remaining number of pending packets in the queue for the node and the received packets at the sink node. It determines the next value of the SO for the nodes in WBSN, as presented in Figure 8. The CDCA has been explained in the three cases, as below:

In the first case, if the pending packets in the queue are greater than the received packets at the sink node this means the traffic is high, and the active period is not enough to transmit the high traffic. The sink node should increase the value of the SO, as shown in Figure 8. Therefore, increasing the SO duration will make more time available for the data transmission in order to deliver the biomedical packets. In addition, the increment of the value in the new SO increases CAP slots or GTS slots based on the priority. If the degree of the priority is high, the number of GTS slots is increased; otherwise, the CAP slots are increased. The coordinated duty cycle (SO/BO) should be adjusted by increasing the value of the next SO. The coordinated duty cycle (CDC) can affect the energy consumption for the nodes in WBSNs.
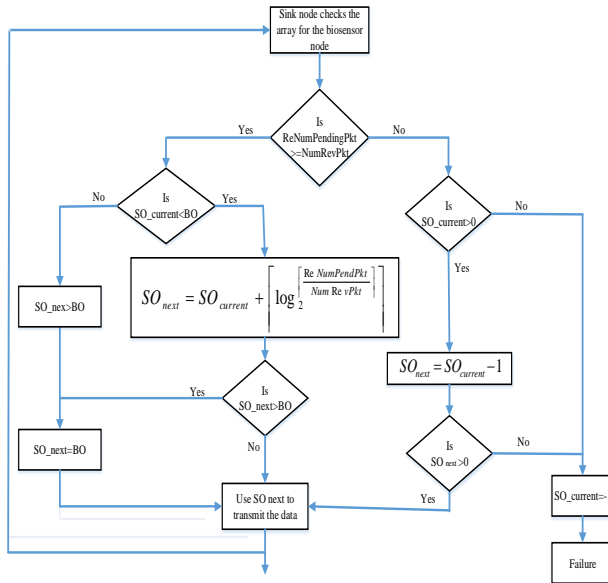
Figure 8. The Coordinated Duty Cycle Algorithm (CDCA)

With respect to the constraints, the calculation of the next SO uses the formula in (5), where *NumPendingPktkt and NumReceivePkt* are the remaining number of pending packets in the queue and the received number of packets at the sink node, respectively.

$$NumPendingPkt > Num\,Re\,ceivePkt \quad and \quad SO < BO$$

$$\rightarrow SO_{next} = SO_{current} + \left\lceil \log 2 \left\lceil \frac{NumPendingPkt}{Num\,Re\,ceivePkt} \right\rceil \right\rceil \quad (5)$$

$$coordinate\,duty\,cycle\,(CDC)_{new} = \beta = \frac{SO_{next}}{BO} \quad (6)$$

The result of the next SO is used to calculate the new coordinate duty cycle (CDC), as shown in equation (6). Then, the new CDC applies the general formula, which is used to compute the energy consumption for the biosensor node in WBSN.

In the second case, if the remaining number of pending packets in the queue is lower than the received packets at the sink node. The constraints are emphasised as shown in (7), and the sink node reduces the active period through decreasing the value of the SO in order to save energy for the biosensor node in WBSN, as illustrated in Figure 8. It determines the next SO and decreases by one, as illustrated in (7). As was mentioned in the previous first case, the next SO is used to calculate the coordinate duty cycle (CDC), as presented in (6). The new CDC will be able to reduce the energy consumption for the biosensor node in WBSN. This approach saves energy and leads to the successful delivery of biomedical packets for nodes in WBSN.

In the third case, if the remaining number of pending packets in the queue is equal to the received packets at the sink node, the sink node maintains the same current value of the SO for the node in WBSN, as presented in (8). Then, the value of CDC is similar to that previous value of CDC.

TABLE III
SHOWS THE VALUES OF THE SPECIFIC PARAMETERS FOR NORDIC NRF2401

Parameter	nRF2401	Parameter	nRF2401
ETXelec	16.7 nJ/bit	Eamp(3.38)	1.97e-9 J/bit
ERXelec	36.1 nJ/bit	Eamp(5.9)	7.99e-6 J/bit

$$NumPendingPkt < Num\,Re\,ceivePkt$$
$$and \quad SO > 0 \quad (7)$$
$$\rightarrow SO_{next} = SO_{current} - 1$$

$$NumPendingPkt = Num\,Re\,ceivePkt \quad (8)$$
$$\rightarrow SO_{next} = SO_{current}$$

D. The implementation CDCA on the proposed design model

With respect to CDCA, the coordinate duty cycle (CDC) is calculated depending on SO and BO values which are affected on the energy consumption for the nodes in WBSNs. The duty cycle achieves energy savings through switching between active and sleep states in the WSN. Let duty cycle is (β), the total energy usage in a time t (period is [0,t]) is given in (9) [27].

$$E_T = t[\beta.E_{txr} + (1-\beta)E_{sleep}] \quad (9)$$

Where E_{txr} is represented the total energy consumption of transmitting and receiving for the node, β is the duty cycle, and E_{sleep} is the energy consumption per second of the sleep state for a sensor node. The sensor nodes remain in active and sleep states with probability β, (1- β) respectively until time t. All nodes are active when the duty cycle (β)=1, indicating that there is no any energy for sleep[27]. The Nordic nRF2401 has low power consumption, it operates in the 2.4-2.45 GHz range, and is commonly used in WSNs[32].

shows the values of the specific parameters for Nordic nRF2401[32]. The range of duty cycle (β) is shown (10), which is applied on the calculation energy formula.

$$0 \le \beta \le 1 \quad (10)$$

With respect to mathematical model for WBSN in [33], which comprises sequences of equations to develop the calculation of energy consumption of biosensor nodes in WBSNs; the concluded equation as shown (11), is used to calculate the energy consumption of WBSN.

$$E^{total}_{whole\_network} = t[(E^t_{TXbr} + E^t_{RXbr} + E^t_{TXrl} + E^t_{TXrs} +$$
$$E^t_{TXbnc} + E^t_{RXbnc} + E^t_{TXrnc} + E^t_{TXncs})] \quad (11)$$

Where the above represents the total energy consumption of transmission of medical data between varied nodes as follows:

E^t_{TXbr} : biosensor nodes to relay nodes
E^t_{TXrl}: relay nodes to other relay nodes,
E^t_{TXrs}: relay nodes to sink node,
E^t_{TXbnc}: biosensor nodes to network coding (NC) relay nodes,
E^t_{TXrnc} : relay nodes to NC relay nodes,
E^t_{TXncs}: NC relay nodes to the sink node,

E_{RXbr}^{t} is the total energy consumption of medical data reception by the simple relay nodes from the biosensor nodes and E_{RXbnc}^{t} is the total energy consumption of medical data reception by the NC relay nodes from the biosensor nodes. Substituting (11) into equation (9), we then obtain

$$E_{T} = t[\beta(E_{TXbr}^{t} + E_{RXbr}^{t} + E_{TXrl}^{t} + E_{TXrs}^{t} + E_{TXbnc}^{t}$$
$$+ E_{RXbnc}^{t} + E_{TXrnc}^{t} + E_{TXncs}^{t}) + (1-\beta)E_{sleep}] \quad (12)$$

As sleeping energy term has amounted smaller value, so equation (13) represents the total energy usage in a time t for nodes in the bottleneck zone WBSN as follows:

$$E_{T} = t[\beta(E_{TXbr}^{t} + E_{RXbr}^{t} + E_{TXrl}^{t} + E_{TXrs}^{t}$$
$$+ E_{TXbnc}^{t} + E_{RXbnc}^{t} + E_{TXrnc}^{t} + E_{TXncs}^{t})] \quad (13)$$

Replacing the terms used (13) by E_{txr} which represents total energy consumption of transmitting and receiving as given in (14) for all nodes in the bottleneck zone WBSN.

$$E_{T} = t[\beta.E_{txr\_nodes\_bottleneck}] \quad (14)$$

E. The numerical energy consumption

We use the same example of the WBSN topology in [33] as shown in Figure 4 because it represents a general case; it includes thirteen biosensor nodes (13) that are placed on the human body. In addition, we use the distance between the biosensor nodes and sink node as in Table I.

In the single-hop approach, the biosensor nodes in the bottleneck zone consume more energy based on the distance such as nodes A, F, and H when compared with other approaches as illustrated in Figure 9. However, in the multi-hop approach, the biosensor nodes relay the packets via the intermediate node towards the sink node. The nodes A, and D have greater energy consumption in the multi-hop but the node C has the same value of energy in most approaches because it is connected directly to the sink node, as shown in Figure 9. The energy consumption for all biosensor nodes in the relay network approach is lower compared with single-hop and multi-hop approach. In addition, simple relay nodes and NC relay nodes are added to the bottleneck zone to reduce the energy consumption for the biosensor nodes based on the network coding approach. It can be observed that energy usage for the nodes B and D is lower when compared with other approaches except that the values of energy consumption for A, F and H are slightly higher than in the relay network approach because energy consumption of these nodes are calculated based on non-line of sight as illustrated in Figure 9.

Looking at Figure 9, it can be seen that the energy consumption for biosensor nodes in the bottleneck zone based on the proposed CDCA tend to have smaller than the energy consumption for nodes in all approaches except node A The duty cycle for node A is equal to one as it requires all time slots and hence no energy saving.
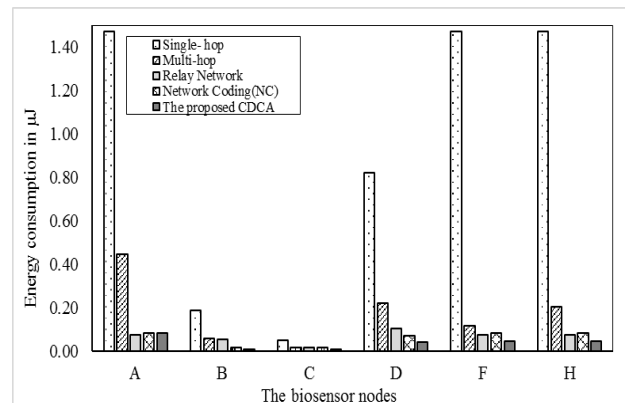

Figure 9. Comparison of energy consumption for biosensor nodes in the bottleneck zone based on the single hop, multi-hop, relay network and Network coding, and the proposed CDCA

F. Energy consumption analysis

With respect to the example of WBSN topology shown in Figure 3, there are some biosensor nodes such as electroencephalogram (K sensor) and ECG (D sensor), EMG (A and I sensor nodes), and blood pressure (G sensor). In addition, we use sequential numbers (1, 2, 3,…, 13) which represent the sequential alphabet for the sensor nodes (A, B, C,…, M), respectively to ease the use of explanatory nodes on WBSN topology.

To analyse the basic performance of the WBSN which consider the theoretical calculation based on the mathematical model as was explained in [33] and compared with applying the CDCA approach on the mathematical model. The results obtained from the preliminary analysis of the energy consumption for the biosensor nodes can be compared in

Figure 10. It can be seen that the energy consumption for biosensor nodes in the CDCA approach tend to have smaller than the energy consumption for nodes in the mathematical model for WBSN without CDCA approach. Although, in both calculations of energy have considered the line of sight (LOS) propagation, the non-line of sight (NLOS) propagation, and the distance between biosensor nodes and sink node.

The results of model used in [33] demonstrate that the energy consumption for biosensor nodes in WBSN model which employs the CDCA has better performance when compare to not using a CDCA as shown in

Figure 10. However, the energy consumption for EMG sensor nodes (which represent nodes 1 and 9) are equal in both calculations as shown in

Figure 10 because the nodes have a high data rate which is 1536 kbps and they need the whole duty cycle which means that the number of slots (SO) is equal to the beacon order (BO). The next section discusses the reliability model.
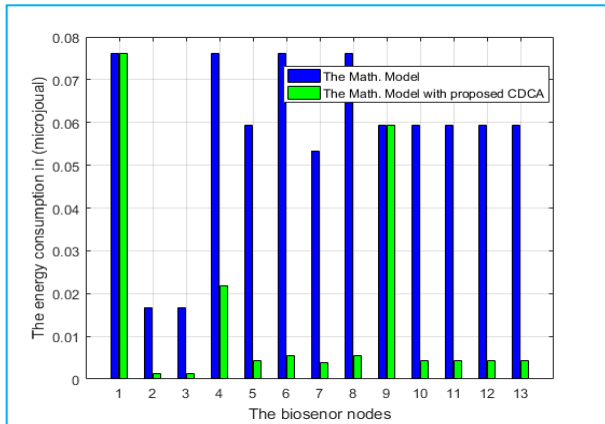
Figure 10. The comparison of energy consumption for biosensor nodes in WBSN based on the mathematical model and the mathematical model with proposed CDCA

VI. The reliability of WBSN model design

A model of a WBSN is represented in Figure 2, which includes one element for each wireless device (biosensor node, simple relay node, NC relay node or sink node) of the network and the number of links (arcs) between them. In order to investigate the transmission reliability of the proposed scheme [17] in Figure 2, with respect to the sample topology of WBSN as shown in Figure 4 (left-hand side), we considered the sample topology to theoretically derive the PSR at the sink node for three approaches such as forwarding, encoding, and combining the forwarding and encoding approaches. Therefore, we study the successful delivery of biomedical packets at the sink node and describe the transmission reliability of the WBSN based on the proposed scheme[17]. Successful delivery, indicates the probability of successful reception (PSR) at the sink node of the biomedical packets transmitted by the biomedical sensor node.

$$p(successful\ delivery) \approx$$
$$\frac{no.\ of\ pktsRec.\ correctly\ by\ sink\ node}{total\ no.\ pktssent\ by\ biosensor\ node} \quad (15)$$

In general, the average bit error probability (p) is calculated based on equations (16) or (17) [34]. The probability of failure (average bit error probability of the link) = p, and the probability of successful reception = (1-p). In most cases, the values $(p_{AR}), (p_{RS}), (p_{AC}), and\ (p_{CS})$ are assumed to be the same for all links in the network. All terms will be defined in the next sections.

$$p_{b_{M-PSK}} \cong \frac{2}{\max(\log_2 M, 2)}$$
$$\sum_{i=1}^{\max(\frac{M}{4}, 1)} Q\left(\sqrt{\frac{2E_b \log_2 M}{N_0}} \quad \sin\frac{(2i-1)\pi}{M} \right) \quad (16)$$

$$p_{b_{M-QAM}} \cong 4\left(\frac{\sqrt{M}-1}{\sqrt{M} \log_2 M} \right)$$
$$\sum_{i=1}^{\sqrt{M/2}} Q\left((2i-1)\sqrt{\frac{3E_b \log_2 M}{N_0(M-1)}} \right) \quad (17)$$

Where:
P_b: the probability of bit-error.
PSK: phase shift keying.
M: number of symbols in the modulation (the modulation order).
E_b/N_0: energy per bit to noise power spectral density ratio.
QAM: quadrature amplitude modulation.

A. Reliability analysis in the forwarding technique

The biosensor node (A) directly transmits the biomedical packets to the sink node (S) through the simple relay node (R) as shown in Figure 11, which represents a sample topology of WBSN using the forwarding approach. The terms, which are used to define the PSR equation at the sink node using the forwarding technique, can be defined as: (p_{AR}) is the average bit error probability of the link from A node to R node; (p_{RS}) is the average bit error probability of the link from R node to S node; $(1 - p_{AR})$ is the probability of successful transmission for link A to R, and $(1 - p_{RS})$ is the probability of successful transmission for link R to S.

With respect to the probability theory, there are two standard rules, which are the addition law and multiplication law [35] as given in Appendix A and are used in this model to compute the PSR at the sink node. In the forwarding technique, the biosensor node (A) sends biomedical packets towards the sink node through the simple relay node. In this case, there are two assumptions depending on how many packets were correctly received at the sink node (S). In the former case, the probability of successful packets being received at the sink node (t=1, 2....m) is between one packet to m packets, and the equation is shown in (18). However, in the latter case, based on the assumption that all biomedical packets (m) are correctly received at the sink node (S), so when t is equal to m in (18), then we calculate the probability of success for all biomedical packets (m) at the sink node (S), which is given in (19).
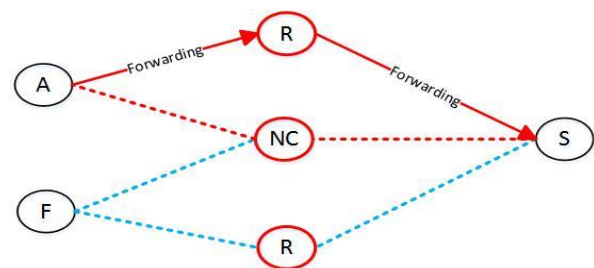

Figure 11. Transmission of biomedical packets from biosensor node to sink node by using forwarding technique in WBSN
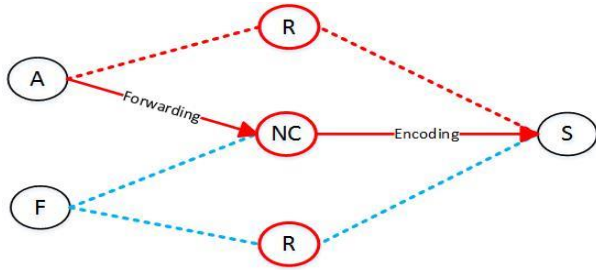
Figure 12. Transmission of biomedical packets from the biosensor node to the sink node using encoding technique in WBSN

$$(1 - p_{AS})_m = \binom{m}{t}\left[(1 - p_{AR})(1 - P_{RS})\right]^t \qquad (18)$$
$$\cdot\left[1 - (1 - p_{AR})(1 - p_{RS})\right]^{m-t}$$

$$(1 - p_{AS})_m = \left[(1 - p_{AR})(1 - P_{RS})\right]^m \qquad (19)$$

B. Reliability analysis in the encoding technique

The biomedical packets are transmitted from the biosensor node (A) to the network coding relay node (NC), and then the NC relay node encodes the biomedical packets to create the encoding packets based on the Galois field technique. These are then transmitted to the sink node (S) as shown in Figure 12, which represents a sample topology for WBSN based on the encoding approach. The terms, which are used to define the PSR at the sink based on the encoding scheme, can be defined as: (p_{AC}) is the average bit error probability of the link from A node to NC node. The (p_{CS}) is the average bit error probability of the link from NC node to S node; the $(1 - p_{AC})$ is the probability of successful transmission for link A to NC, and the $(1 - p_{CS})$ is the probability of successful transmission for link NC to S.

As far as the encoding scheme is concerned, there are two transmission parts in the encoding technique. Firstly, there is the forwarding transmission, which transmits biomedical packets (m) from the biosensor node (A) towards the NC node. Secondly, there is the encoding transmission, which encodes the biomedical packets (m') and transmits them towards the sink node (S). With the encoding transmission,
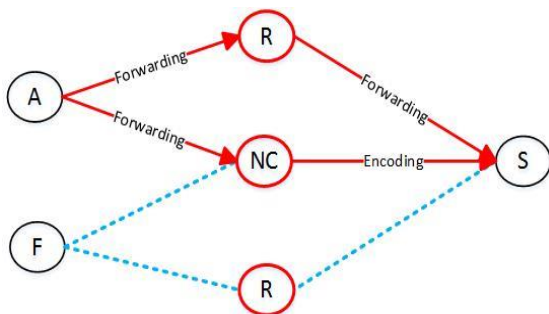

Figure 13. Transmission of biomedical packets from biosensor node to sink node using Combination technique

the PSR at the NC node for biomedical packets can be given in (20), assuming that the probability of the links are independent. We assume that all received packets (m) at the NC relay node are correct. The PSR is represented in (21) at the NC node. In this case, the number of transmission packets is equal to the number of received packets.

$$(1 - p_{AC})_{i\ from\ m} = \binom{m}{i}(1 - p_{AC})^i\ p_{AC}^{m-i} \qquad (20)$$

$$(1 - p_{AC})_{i\ from\ m} = (1 - p_{AC})^m \qquad if\ i = m \qquad (21)$$

The PSR for encoding biomedical packets at the sink node (S) is given in (22). Furthermore, the sink node (S) needs to receive at least m coded packets from the NC relay node (C) to be able to recover the original information. The sink node (S) should receive biomedical packets greater than or equal to m packets, which are transmitted from the biosensor node (A). This means that the number of encoded packets should be greater than or equal to the number of native packets that help to recover the original packets in the sink node (S). The relationship between the encoded packet and the native packets is given in (22). The PSR for the biomedical packets, which are correctly received at the sink node, are represented in (23).

$$(1 - p_{CS})_{en} = \sum_{i=m}^{m'} \binom{m'}{i}(1 - p_{CS})^i\ p_{CS}^{m'-i} \qquad (22)$$
$$m' \ge m$$

$$(1 - p_{AC})(1 - p_{CS})_{fen} =$$
$$(1 - p_{AC})^m \sum_{i=m}^{m'} \binom{m'}{i}(1 - p_{CS})^i\ p_{CS}^{m'-1} \qquad (23)$$

In the formula above the forwarding part (from biosensor node to the NC relay node) is represented as well as the encoding part (from the NC relay node to the sink node). Here, m represents native packets (original packets) from the biosensor node (S) to the NC relay node (C) and m' represents encoding packets, which are transmitted from NC relay node (C) to the sink node (S). The derived expression of the encoding technique for nodes in the bottleneck zone is given in Appendix A.

C. Reliability analysis of the combined technique

The combined technique is a term used to combine the forwarding technique and encoding technique as shown in Figure 13, which represents a sample topology for WBSN depending on the combined approach. The biosensor node (A) sends the duplicated biomedical packets to the simple relay node (R) and the NC relay node (C) and then towards the sink node (S). With regard to the serial and parallel reliability rules [35] in Appendix A, these rules of reliability are applied to totally calculate the PSR at the sink node based

IEEE *Access*

Multidisciplinary : Rapid Review : Open Access Journal

on the combined technique, which includes the forwarding technique and encoding techniques respectively, as given in (24) and (25). The PSR at the sink node (S) can be seen in (27) based on the combined scheme. We also apply the rules for the reliability in Appendix A to compute the total PSR at the sink node as shown in (26) based on the combined scheme. Finally, we use (26) to calculate the total PSR at the sink node based on (18) and (23), which is represented in (27).

$$p(fo\_successful) = p(AR \cap RS) \qquad (24)$$

$$p(en\_successful) = p(AC \cap CS) \qquad (25)$$

$$
\begin{aligned}
p(co\_successful) &= p[(AC \cap CS) \cup (AC \cap CR)] \\
&= p(AR).p(RS) + p(AC).p(CS) \\
&= p(AR).p(RS) + p(AC).p(CS) \\
&\quad -[p(AR).p(RS).p(AC).p(CS)] \\
&= p_{AR}.p_{RS} + p_{AC}.p_{CS} - [p_{AR}.p_{RS}.p_{AC}.p_{CS}]
\end{aligned}
\qquad (26)
$$

$$
\begin{aligned}
&(1-p)_{ARS} \cup (1-p)_{ACS} = \\
&\binom{m}{t}[(1-p_{AR})(1-P_{RS})]^t [1-(1-p_{AR})(1-p_{RS})]^{m-t} + \\
&(1-p_{AC})^m \sum_{i=m}^{m'} \binom{m'}{i}(1-p_{CS})^i p_{CS}^{m'-1} - \\
&\left[\begin{matrix} \binom{m}{t}[(1-p_{AR})(1-P_{RS})]^t [1-(1-p_{AR})(1-p_{RS})]^{m-t} \\ .(1-p_{AC})^m \sum_{i=m}^{m'} \binom{m'}{i}(1-p_{CS})^i p_{CS}^{m'-1} \end{matrix} \right]
\end{aligned}
\qquad (27)
$$

D. The numerical PSR for Sample topology of WBSN
As far as the encoding approach is concerned, we have analysed the effect of the number of coded biomedical the packets on the PSR at the sink node. It is essential that the sink node receives at least m coded biomedical packets from NC relay node to be able to recover the original biomedical packets because the decoding of the biomedical packets depends on the operations, which are performed at the network coding relay node. The probability of successful reception (PSR) at the sink node as a function of the (E_b/N_0) for varied numbers of coded biomedical packets (10,11, & 15) is shown in Figure 14.The results of this study indicate that an increase of coded biomedical packets will lead to an increase in the probability of successful reception at the sink node, as shown in Figure 14. With respect to RLNC, which is employed in this approach, increasing the number of the encoded biomedical packets achieves better performance in terms of PSR and (Eb/N0) and improves network reliability as shown in Figure 14. For instance, we notice that the PSR for 15 coded biomedical packets is better than 10 packets.

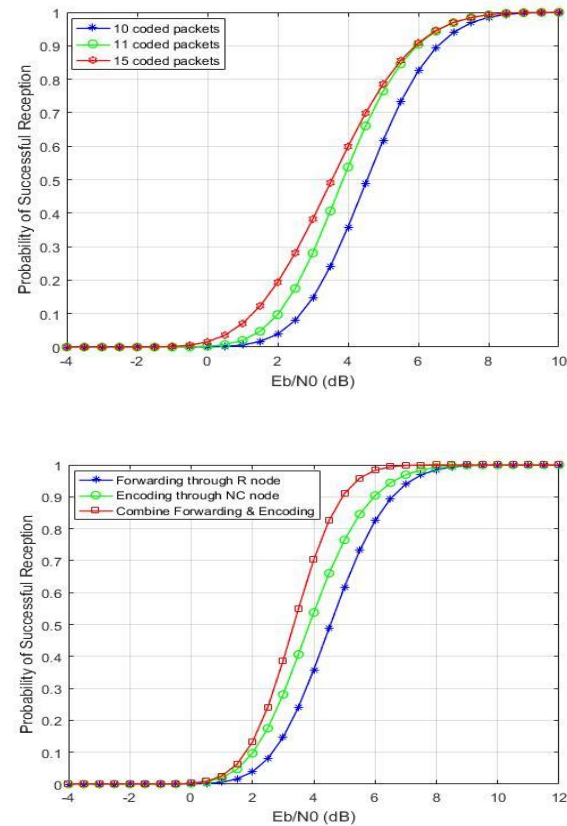**Figure 14. Probability of success Vs SNR**

Figure 15. Comparison of the PSR at sink node in the three techniques: the forwarding, encoding, and combined technique

The reliability of WBSN for the three techniques as shown in Figure 15 is investigated against the energy to noise ratio (Eb/N0), which is the energy per bit to noise power spectral density ratio. Figure 15. shows the probability of successful reception (PSR) at the sink node as a function of the energy per bit to noise power spectral density ratio (E_b/N_0) for biomedical packets in the forwarding, encoding, and combined technique. Notice that the encoding technique offers a better performance than the forwarding technique in terms of PSR at the sink node; the encoding technique requires lower energy per bit than the forwarding technique. In Figure 15, also shows that the combined approach (forwarding and encoding) can achieve better reliability performance than other approaches. Also, it should be noted that the combined approach based on RLNC offers a better performance than other approaches in the probability of achieving successful reception at the sink node. The combined technique also has the best performance with lower energy consumption per bit than the other techniques. For example, the combined technique requires about 6.1 dB less than the encoding and forwarding technique to achieve better performance of PSR ($PSR \approx 1$) as shown in Figure 15.

E. Comparing the proposed scheme with existing scheme
The encoding technique proposes and presents a WBSN based on RLNC, which improves the PSR at the sink node.

Figure 16 shows the PSR at the sink node as a function of the energy per bit to noise power spectral density ratio (E_b/N_0) for the RLNC scheme and the XOR NC scheme. The value of PSR at the sink node using RLNC scheme and the XOR NC scheme increase with the energy per bit to noise power spectral density ratio (E_b/N_0).

Moreover, we discuss the performance of the encoding scheme, which employs RLNC and existing technique, which uses the XOR NC scheme in terms of PSR at the sink node, reliability, and average energy per bit. Figure 16 shows an overview of the PSR at the sink node for RLNC technique (proposed scheme) and XOR NC technique. Notice that the proposed RLNC encoding technique offers better performance and better reliability than the XOR NC technique. Moreover, the encoding technique provides a higher PSR at the sink node than the XOR NC technique. For example, when the value of (E_b/N_0) is 5.5 dB, the value of the PSR at the sink node is 0.715 and 0.845 for the XOR NC scheme and RLNC scheme, respectively, as shown in Figure 16. In [28], the authors showed that the XOR NC technique reduces the packet delivery ratio. However, the RLNC technique enhances the reliability of data delivery. In summary, the results show that the proposed scheme outperforms the XOR NC scheme in terms of reliability and PSR at the sink node, which is related to lower power consumption.

F. Measurement methods

In order to calculate the accuracy for the improvement between the three approaches, we use Kolmogorov-Smirnov test (K-S test) and trapezium rule.

1) MEASUREMENT OF THE IMPROVEMENT BASED ON K-S TEST

The Kolmogorov-Smirnov test (K-S test) attempts to determine if two data sets differ significantly. It has the advantage of making no assumptions about the distribution of data [36]. As regards the K-S test, it is used to measure the accuracy of the improvement for the PSR at the sink node in the three approaches, which compares two samples, and is used to find the different distributions in the samples. In Figure 17, we apply K-S test to the results of Figure 15. The graph area is divided into three areas, where the first and third area represent the censoring data, which is the difference between two samples approximately equal to zero. We consider the data set in the second area between them, and use the K-S test to determine the bigger difference between two samples distribution. Moreover, it can be seen from the Figure 17, the combined approach is consistently better than the other approaches.

According to K-S test, the accuracy of the improvement in the PSR at the sink node for the comparison of encoding approach with the forwarding approach are shown in Figure 18 along with the comparison of the combined approach with the forwarding approach, and the comparison of combined approach with encoding approach are 0.1792, 0.3449, and 0.1658, respectively.
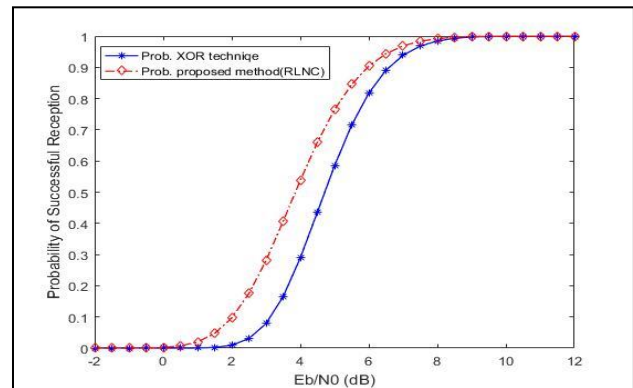

Figure 16. Comparison of the PSR at the sink node based on the encoding technique (RLNC) and XOR NC technique

2) MEASUREMENT OF THE IMPROVEMENT BASED ON TRAPEZIUM RULE

There is another method to measure the improvement percentage points (points change) of the PSR at the sink node. The trapezium rule [37] is a way of estimating the area under or above the curve, and it gives a method of estimating the numerical integration quadrature. In Figure 19 we apply trapezium rule to the results in Figure 15. The ideal fit is 100% and the worst possible fit is 0%, so the combined technique is better than the encoding technique, which is better than the forwarding technique. Moreover, there is not a curve cross in the experimental range (-4, 12). As can be seen from Figure 19, the combined technique is consistently better than the encoding technique and the encoding technique is consistently better than the forwarding technique.

The trapezium rule is used to calculate the area under the curve based on the formula (28), which uses two value points, as shown in Figure 19. Then, the equation (29) is applied to compute the percentage of the improvement for the probability. With respect to trapezium rule, the areas and the percentages are calculated for the three techniques, as shown in

Table IV. On the other hand, the formula (30) is also used to compute the areas above the curves, and more details about the areas and the percentages are shown in Table V. The percentages of the improvement in the probability for success at the sink node are matched for the above and below calculations.

$$area = \frac{1}{2}\left(\frac{y_1 + y_2}{2}\right) \quad (28)$$

$$percentage(\%) = \left(\frac{area}{16}\right) * 100 \quad (29)$$

$$area = \frac{1}{2}\left\{\frac{(1-y_1) + (1-y_2)}{2}\right\} \quad (30)$$

The bar chart illustrates the improvement percentage change for the PSR at sink node for all approaches as shown in Figure 20. It can be seen that the improvement percentage

IEEE *Access*
Multidisciplinary : Rapid Review : Open Access Journal

of the combined approach to the forwarding approach is 7.66%, and this is a significant improvement. However, the improvement percentage of the combined approach to the encoding approach is 3.59%, and improvement percentage of the encoding approach to the forwarding approach is 4.07%.
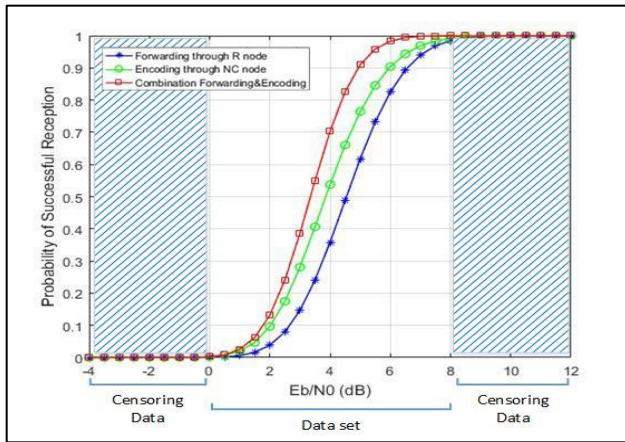

Figure 17. The data set which uses Kolmogorov-Smirnov test (K-S test to measure the accuracy of improvement for the PSR in three approaches)
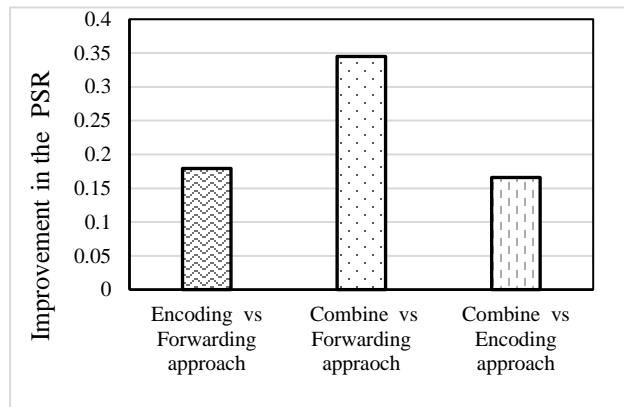

Figure 18. The accuracy of the improvement for the PSR at sink

TABLE IV
THE AREAS AND PERCENTAGES FOR THE THREE TECHNIQUES BASED ON THE UNDER CURVE FORMULA

	Area for the forwarding technique	Area for the encoding technique	Area for the combined technique
Area	7.4151	8.0661	8.6414
Percentage (%)	46.3445	50.4134	54.0091

TABLE V
THE AREAS AND THE PERCENTAGES FOR THE THREE TECHNIQUES BASED ON ABOVE CURVE FORMULA

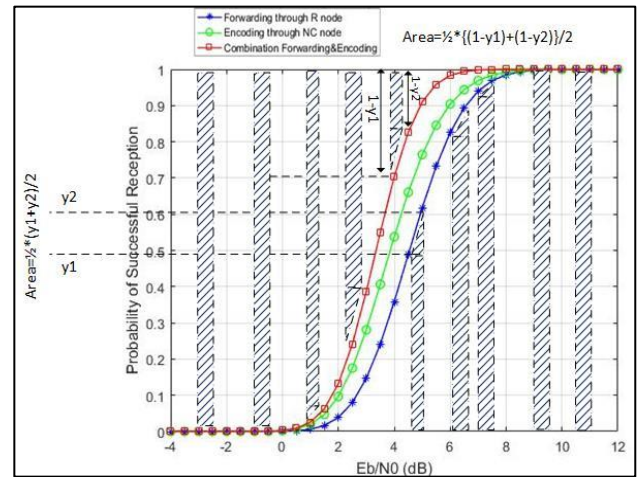|	Area for the forwarding technique	Area for the encoding technique	Area for the combined technique
Area	8.5848	7.9338	7.3585
Percentage (%)	53.6554	49.5865	45.9908
Fit=100- Percentage %	46.3445	50.4134	54.0091

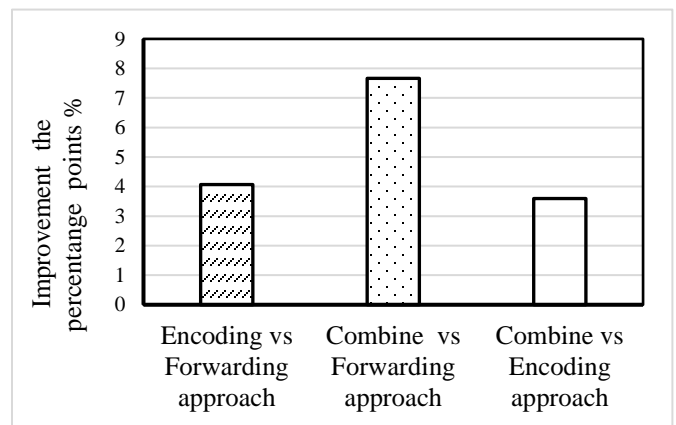Figure 19. The trapezium technique used to calculate the areas

Figure 20. Comparison of the improvement percentage for three techniques

VII. SIMULATION

The simulation is implemented to validate the proposed CDCA and reliability in WBSN. The proposed approach deploys 13 biosensor nodes on the human body with a sink node, which is also placed on the body. In addition, relay nodes are deployed on the body using 250 Kbps data rate; to assist the biosensor nodes through data transmissions and receptions, in addition to which some of them apply NC technique. The body sensor network adopts IEEE 802.15.4 protocol, which operates at the 2.4 GHz frequency. With respect to the MAC configuration in this protocol, the standard values for SO and BO are used to represent the initial values which are then changed depending on the priority of the biosensor nodes data and the behaviour of traffic in the WBSN. Also, MPDU (MAC Protocol Data Unit) contains MAC header (the range is 7-23 byte), MAC Payload, and MAC footer (2 byte). The length of the symbol is 16 bit, the symbol duration is 16us, the sampling frequency is 50 frame/second, and each slot is 60 symbols.

The parameters are given in Table III for the Nordic nRF2401 in 2.4-2.45 GHz which are used in the design

scenarios using Matlab. Moreover, the path loss coefficient (n) which have LOS=3.38 or NLOS=5.9 is used. Also, Galois Field operations are used.

A. Studied scenario: energy consumption for the bottleneck zone nodes with CDCA

The sink node allocates the GTS slots to the biosensor nodes, which provide accurate biomedical data about the patient. The priority of the biosensor node represents by one bit, if high priority it is one and if low priority it is zero, in our system.

In this section, we consider the biosensor nodes in the bottleneck zone, which include the EMG sensor (node 1), the body temperature sensor (node 2), the pulse rate sensor (node 3), the ECG sensor (node 4), the glucose monitor sensor (node 6), and the blood pressure monitor (node 8). The proposed CDCA WBSN has been implemented in the scenarios which can happen, as below:

We select random priority and active status for the nodes in the WBSN as shown in Table VI, where the proposed CDCA with the model for WBSN has been implemented in the three scenarios which can happen, as below:

In the first scenario, we show the comparison for the energy in the mathematical model situation and the simulation for nodes in the bottleneck zone based on CDCA. The energy usage for nodes in the experiment is more than in the mathematical model as illustrated in Fig. 21(a) because the summation for the number of GTS slots and CAP in the simulation is higher than the slots in the mathematical model, as shown in Fig. 21(b). The sink node allocates the number of GTS slots for the biosensor nodes, which need to send biomedical packets under the priority condition, whereas the sink node allocates the number of CAP slots to other nodes. For example, in the simulation, the number of GTS slots is eight and the CAP slots number is five, while the total slots are thirteen as shown in Fig. 21(b), which latter is greater than the number of slots in the mathematical model (4 GTS+4 CAP). Then, we calculate the duty cycle (DC) for the nodes, which represents the ratio between the total of the slots (SO) and the Beacon Order (BO).

In the second scenario, we use the same setting as in the first scenario except that the number of pending packets in the queue is equal to the number of received packets at the sink node. It is apparent from Fig. 22(a) that the energy for nodes in the bottleneck zone is equal in both calculations.

TABLE VI
INFORMATION OF PRIORITY AND ACTIVE STATUS FOR THE NODE IN THE BOTTLENECK ZONE WBSN

	EMG	body temperature	Pulse rate	ECG	Glucose monitor	Blood pressure
Node no.	1	2	3	4	6	8
Priority	0	1	1	0	1	1
Active	0	1	1	1	1	1

Furthermore, the number of slots is equal in the two cases, as illustrated in Fig. 22(b).

In the third scenario, the number of pending packets in the queue is less than the number of received packets at the sink node. From the chart, as shown in Fig.23(a), it can be seen that energy consumption in the simulation is lower than the energy consumption for nodes in the mathematical model because the value of the duty cycle for nodes in the simulation is less than in the mathematical model. Furthermore, the total number of slots in the simulation is seven whereas the slots in the mathematical model number are eight, as presented in Fig. 23(b).

B. Studied scenario: reliability for the bottleneck zone nodes in WBSN

The analysis results for the proposed technique (RLNC) and XOR NC are approximately matched with the simulation results for the encoding technique (RLNC) and XOR NC scheme, as shown in Figure 24. We have compared the proposed technique (encoding technique) to other techniques, such as forwarding scheme that do not use any type of network coding family and combined technique mixes two techniques; the first technique does not use network coding and the second technique employs network coding. Each scheme has a special strategy for the calculation of the probability, which was described in Section V.

The simulation results were obtained through the simulation using MATLAB software, where the number of biosensor nodes is fixed, as well as the number of relay nodes. We assume that the sensor node has ten packets, all links have the same energy per bit to noise power spectral density ration, and they add white Gaussian noise (AWGN) on the channel. The Galois field $GF(2^8)$ is used for the network coding operations and random coefficients to create the encoding packets.

The PSR at the sink node is represented as a function of the (E_b/N_0) for biomedical packets in all approaches, which transmits the original packets (m) and encoded packets (m'). The encoding technique should always transmit at least $m+1$ coded packets to have a better performance than the forwarding technique, as shown in Figure 25. It should be noted that, the encoding technique employs RLNC, which requires lower energy per bit than the forwarding technique. In addition, the encoding technique (the derived expression as given in Appendix A) has a better performance than the forwarding technique in terms of the PSR at the sink node, and PSR increases dramatically until it reaches to one in the encoding scheme (proposed scheme). Also, the reliability for the proposed scheme is higher than the reliability for the forwarding scheme. Moreover, overall, the combined scheme has a higher performance than the forwarding and encoding schemes.

The analysis results are approximately matched with the simulation results for these schemes. We simulated the

a: The comparison of energy consumption for biosensor nodes in the bottleneck zone in the mathematical model and the simulation based on CDCA when the no. of pending packets is a greater than the no. received packets

b: The comparison for the number of GTS slots and CAP slots in the mathematical model and the simulation for biosensor nodes in the bottleneck zone based on CDCA, when the no. of pending packets is a greater than the no. of received packets
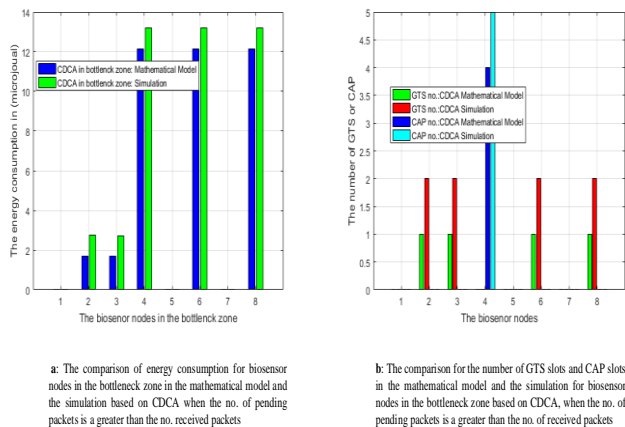
Figure 21. Comparison of the energy consumption, and GTS and CAP slots for nodes in the bottleneck zone in the mathematical model and simulation based on CDCA with no. of pending packets greater than the no. received packets

a: The comparison of energy consumption for biosensor nodes in the bottleneck zone in the mathematical and the simulation based on CDCA when the no. of pending packets is an equal to the no. received packets

b: The comparison for the number of GTS slots and CAP slots in the mathematical model and the simulation for biosensor nodes in the bottleneck zone based on CDCA, when the no. of pending packets is an equal to the no. of received packets
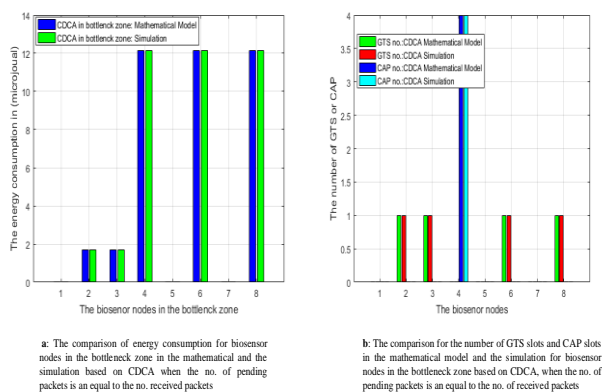
Figure 22. Comparison of the energy consumption, and GTS and CAP slots for nodes in the bottleneck zone in the mathematical model and simulation based on CDCA with no. of pending packets equal to the no. received packets
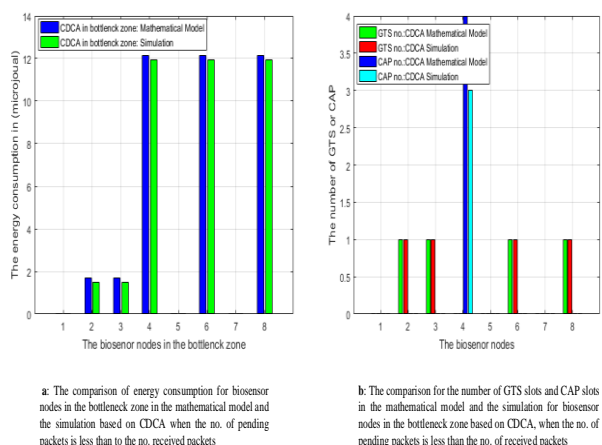

a: The comparison of energy consumption for biosensor nodes in the bottleneck zone in the mathematical model and the simulation based on CDCA when the no. of pending packets is less than to the no. received packets

b: The comparison for the number of GTS slots and CAP slots in the mathematical model and the simulation for biosensor nodes in the bottleneck zone based on CDCA, when the no. of pending packets is less than the no. of received packets

Figure 23. Comparison of the energy consumption, and GTS and CAP slots for nodes in the bottleneck zone in the mathematical model and simulation based on CDCA with no. of pending packets less than the no. of received packets
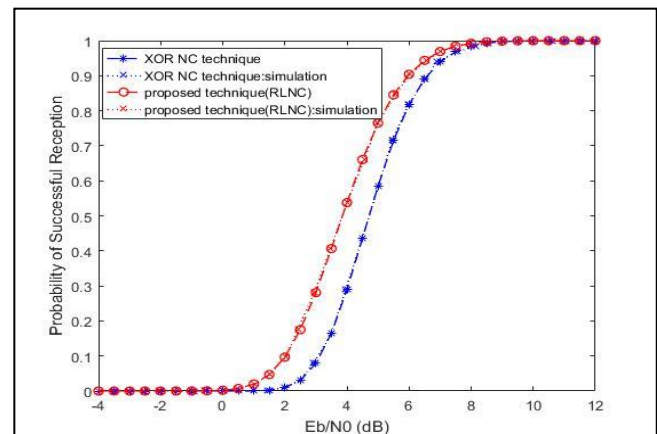

Figure 24. Comparison of the analysis and simulation results for the PSR at the sink node based on the encoding technique and XOR NC technique
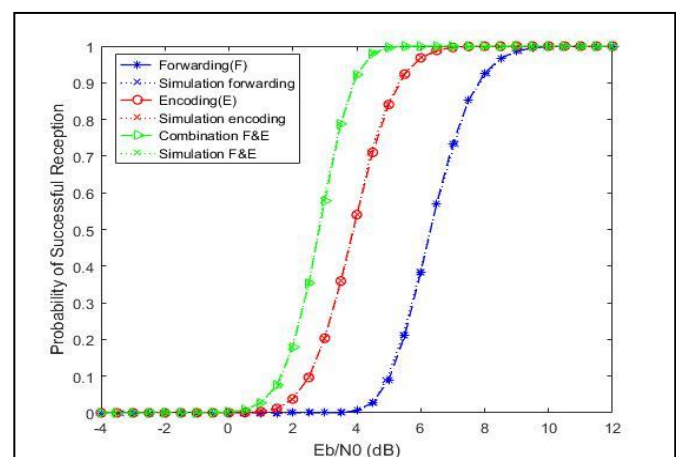

Figure 25. Comparison of the analysis and simulation results of the PSR at the sink node based on all the schemes for the nodes in the bottleneck zone WBSN, which use 10 packets

influence of a number of biomedical packets, which are employed to calculate the PSR at the sink node on those schemes such as forwarding, encoding (proposed scheme), and combining them.

VIII. Conclusions

In this paper, the problems of high energy usage and lost biomedical packets in the bottleneck zone in WBSNs have been considered. . The Coordinate Duty Cycle Algorithm (CDCA) design is proposed for WBSNs; it was selected correctly based on the real behaviour of traffic and the priority of the sensor nodes in WBSNs. In addition, a mathematical model[33] has been developed for the enhancement of the design and energy efficiency of wireless body area networks through applying the proposed CDCA approach. The combination of the CDCA and RLNC approaches is applied to reduce the energy consumption for nodes and improve the transmission reliability in the bottleneck zone. Moreover, the

results of our approach show that reducing energy usage compared to existing techniques is possible. This reduces the energy consumption for biosensor nodes, as required; RLNC showed significant advantages over the XOR NC in terms of reliability and probability of successful reception at the sink node, which is related to lower power; it is clear that RLNC can be employed to improve the reliability of WBSNs. We derived an expression for the encoding approach of the PSR at the sink node and found that network coding significantly improves the reliability of WBSNs. Our numerical and simulation results indicate that the proposed encoding method, which employs RLNC, provides a higher PSR at the sink node than the XOR NC technique.

X. APPENDIX

Appendix A.
The basic information about some laws of probability Theorem 1[39]:

In general, when two events A and B are termed to be independent of each other, meaning that the probability of one event occurring does not change the probability that the other event occurs. In [39], the events A and B are independent if

$$P(A \cap B) = P(A)P(B) \qquad (31)$$

If there are events such as A_1, A_2, A_3,……A_i which are independent, the joint probability of the these sets is the product of their probabilities. Also, the serial system reliability is the product of the independent subsystem reliabilities. In general, a family $\{A_i : i \in I\}$ is called independent if

$$P\left(\bigcap_{i \in J} A_i\right) = \prod_{i \in J} P(A_i) \qquad (32)$$

For all finite subsets J of I.

More explanation about (31), when A and B are said to be independent events, if and only if the probability of A and B occurring simultaneously is equal to the product of their probabilities [40].

$$P(A \cap B) = P(A)P(B)$$

Definition: $\qquad\qquad\qquad\qquad\qquad (33)$
if A and B are independent events
$$P(A|B) = P(A) \quad \text{and} \quad P(B|A) = P(B)$$

This definition is often called multiplication rule [40].

Theorem 2[40]:

In [40], the addition law of probability is described as given in (34); the probability of either A or B, or both occurring in the probability of A plus the probability of B, minus the probability that they both occur. If two events are A and B then:

$$P(A \cup B) = P(A) + P(B) - P(A \cap B) \qquad (34)$$

Where $P(A \cap B)$ is explained in (31) and (33).

Theorem 3 [40]: Binomial distribution

In [40], authors assumed that x is represented as a random variable, where n is a positive integer, and where p is a real number between zero and one ($0 < p < 1$). The probability of x "success" in n independent trials and $(n-x)$ "failure" is given by (35) which represents the binomial distribution [40].

$$p_X(x) = \binom{n}{x} p^x (1-p)^{n-x} \qquad x = 0,1,......,n \qquad (35)$$
$$= 0 \qquad\qquad\qquad \text{Otherwise}$$

Where p is the probability of an individual "success"; $\binom{n}{x}$ is the binomial coefficient which represents the number of ways in which the x "successes" can occur in the n trials.

$$\binom{n}{x} = \frac{n!}{x!(n-x)!} \qquad (36)$$

General rule 4: The probability for success for the packets

The biosesnor nodes are connected with other nodes such as biosensor nodes, relay nodes, and NC relay nodes in the network of WBSN. We describe the assumption for all nodes, which are an average bit error probability and successful probability.

As a general rule, the probability for success for the packets, which are transmmitted toward the sink node through relay node:

Let x is a node
Let (p_{XR}) be average bit error probability
of the link from X node to R node
Let (p_{RS}) average bit error probability of
the link from R node to S node
So that, $\qquad\qquad\qquad\qquad (37)$
Let $(1 - p_{XR})$ is the probability of success
for link X to R
Let $(1 - p_{RS})$ is the probability of success
for link R to S

As a general rule, the probability for success for the packets, which are transmmitted toward the sink node through network coding relay node:

Let x is a node
Let (p_{XC}) be average bit error probability
of the link from X node to C node $\qquad (38)$
Let (p_{CS}) average bit error probability of
the link from C node to S node
So that,

Let $(1 - p_{XC})$ is the probability of success for link X to C

Let $(1 - p_{CS})$ is the probability of success for link C to S

5: Analysis of the encoding technique (proposed scheme) for the nodes in the bottleneck zone WBSN

The total of PSR at the sink node is computed as given in (39) based on the encoding technique. Each node transmits packets toward the sink node through the network coding node (D), which generates the encoding packets. The topology WBSN in this technique is shown in Figure 26. The NC relay node should receive at least m linearly independent packets, eith m' representing the encoding packets. The probability for success of the bottleneck zone is calculated as given in (39).

$$p(encode\_successful) = 1 - p(encode\_failure)$$
$$= 1 - [p(failure_{AFCS}) . p(failure_{BS})$$
$$. p(failure_{Cbio}) . p(failure_{DHCS})] \tag{39}$$

Where

$$p(failure_{AFCS}) = 1 - p(successful_{AFCS})$$
$$= (1 - p_{AC})^m . (1 - p_{FC})^m$$
$$. \sum_{i=m}^{m'} \binom{m'}{i} (1 - p_{CS})^i . p_{CS}^{m'-i} \quad \text{where } m' \geq m \tag{40}$$

The proability of failure for node B and Cbio are shown in (41) and (42), respectively.

$$p(failure_{BS}) = \binom{m}{t} p(failure_{BS})^{m-t} . (1 - p(failure_{BS}))^t$$
$$p(failure_{BS}) = \binom{m}{t} p_{BS}^{m-t} . (1 - p_{BS})^t \tag{41}$$

$$p(failure_{CbioS}) = \binom{m}{t} p(failure_{CbioS})^{m-t}$$
$$. (1 - p(failure_{CbioS}))^t$$
$$p(failure_{CbioS}) = \binom{m}{t} p_{CbioS}^{m-t} . (1 - p_{CbioS})^t \tag{42}$$

The proability of failure for $p(failure_{DHCS})$ is shown in (43).

$$p(failure_{DHCS}) = 1 - p(successful_{DHCS})$$
$$p(successful_{DHCS}) = (1 - p_{DC})^m . (1 - p_{HC})^m$$
$$. \sum_{i=m}^{m'} \binom{m'}{i} (1 - p_{CS})^i . p_{CS}^{m'-i} \quad \text{where } m' \geq m \tag{43}$$
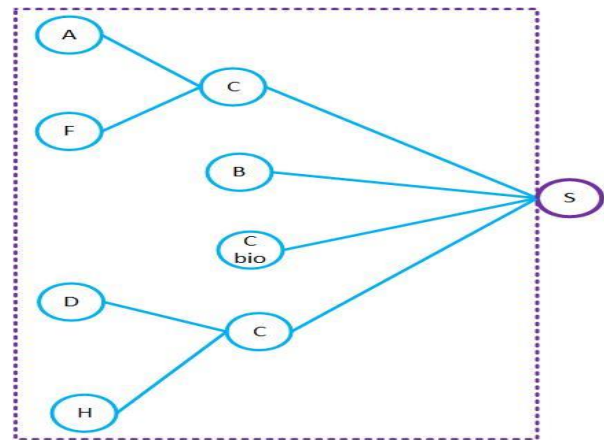

Figure 26: The topology for the nodes in the bottleneck zone based on the encoding technique

Reference

[1] K. M. S. Thotahewa, J.-M. Redoute, and M. R. Yuce, *Ultra Wideband Based Wireless Body Area Networks*. New York: Springer Science & Business, 2014..

[2] M. Iftikhar, N. Al Elaiwi, and M. S. Aksoy, "Performance Analysis of Priority Queuing Model for Low Power Wireless Body Area Networks (WBANs)," *Procedia Comput. Sci.*, vol. 34, pp. 518–525, 2014.

[3] R. Ahlswede, N. Cai, S.-Y. R. Li, and R. W. Yeung, "Network Information Flow," *IEEE Trans. Inf. Theory*, vol. 46, no. 4, pp. 1204–1216, 2000.

[4] T. Ho, R. Koetter, M. Medard, D. R. Karger, and M. Effros, "The benefits of coding over routing in a randomized setting," *IEEE Int. Symp. Inf. Theory, 2003. Proceedings.*, p. 7803, 2003.

[5] T. Ho, M. Médard, J. Shi, M. Effros, and D. R. Karger, "On randomized network coding," *Proc. Annu. Allert. Conf. Commun. Control Comput.*, vol. 41, no. 1, pp. 11–20, 2003.

[6] S. Pfletschinger, M. Navarro, and C. Ibars, "Energy-efficient data collection in WSN with network coding," *2011 IEEE GLOBECOM Work. GC Wkshps 2011*, pp. 394–398, 2011.

[7] M. V Funde, M. A. Gaikwad, and P. A. W. Hinganikar, "Review of Lifetime Enhancement of Wireless Sensor Networks," vol. 2, no. 2, pp. 35–39, 2015.

[8] J. Jeon, W. L. Jong, Y. H. Jae, and H. K. Wook, "DCA: Duty-cycle adaptation algorithm for IEEE 802.15.4 beacon-enabled networks," in *IEEE Vehicular Technology Conference*, 2007, pp. 110–113.

[9] J. H. Lim and B. T. Jang, "Dynamic duty cycle adaptation to real-time data in IEEE 802.15.4 based WSN," *2008 5th IEEE Consum. Commun. Netw. Conf. CCNC 2008*, pp. 353–357, 2008.

[10] B. Gao and C. He, "An individual beacon order adaptation algorithm for IEEE 802.15.4 networks," *2008 11th IEEE Singapore Int. Conf. Commun. Syst. ICCS 2008*, pp. 12–16, 2008.

[11] Y. Gadallah and M. Jaafari, "A Reliable Energy-Efficient 802.15.4-Based MAC Protocol for Wireless Sensor Networks," *Wirel. Commun. Netw. Conf. (WCNC), 2010 IEEE*, pp. 1–6, 2010.

[12] R. De Paz Alberola and D. Pesch, "Duty cycle learning algorithm (DCLA) for IEEE 802.15.4 beacon-enabled wireless sensor networks," *Ad Hoc Networks*, vol. 10, no. 4, pp. 664–679, 2012.

[13] J. Hurtado-lópez and E. Casilari, "An Adaptive Algorithm to Optimize the Dynamics of IEEE 802.15.4 Networks," *Mob. Networks Manag.*, no. 2, pp. 136–148, 2013.

[14] P. Pelegris and K. Banitsas, "Investigating the efficiency of IEEE 802.15.4 for medical monitoring applications," *Proc. Annu. Int. Conf. IEEE Eng. Med. Biol. Soc. EMBS*, pp. 8215–

8218, 2011.

[15] C. H. S. Oliveira, Y. Ghamri-Doudane, and S. Lohier, "A duty cycle self-adaptation algorithm for the 802.15.4 wireless sensor networks," *Glob. Inf. Infrastruct. Symp. GIIS 2013*, 2013.

[16] and H. F. R. Hadi Rasouli, Yousef S. Kavian, "ADCA : Adaptive Duty Cycle Algorithm for Energy Wireless Sensor Networks," *IEEE Sens. J.*, vol. 14, no. 11, pp. 3893–3902, 2014.

[17] H. Alshaheen and H. Takruri Rizk, "Improving the Energy Efficiency for a WBSN based on a Coordinate Duty Cycle and Network Coding," in *2017 13th International Wireless Communications and Mobile Computing Conference (IWCMC)*, pp. 1215–1220.

[18] Z. J. Haas and T.-C. C. T.-C. Chen, "Cluster-based cooperative communication with network coding in wireless networks," *Mil. Commun. Conf. 2010 - Milcom 2010*, pp. 2082–2089, 2010.

[19] M. R. Wsns, X. Liu, S. Member, X. Gong, and Y. Zheng, "on Random Network Coding in," vol. 14, no. 8, pp. 2514–2523, 2014.

[20] G. E. Arrobo and R. D. Gitlin, "Improving the reliability of wireless body area networks," *2011 Annu. Int. Conf. IEEE Eng. Med. Biol. Soc.*, pp. 2192–2195, 2011.

[21] G. Arrobo and R. Gitlin, "New approaches to reliable wireless body area networks," *... , Commun. Antennas ...*, pp. 2–7, 2011.

[22] G. E. Arrobo and R. D. Gitlin, "Minimizing energy consumption for cooperative network and diversity coded sensor networks," *Wirel. Telecommun. Symp.*, 2014.

[23] M. A. Samaneh Movassaghi, Mahyar Shirvanimoghaddam, "A Cooperative Network Coding Approach to Reliable Wireless Body Area Networks with Demodulate-and-Forward," pp. 394–399, 2013.

[24] S. L. S. Lee and H. S. Lee, "Analysis of Network Lifetime in Cluster-Based Sensor Networks," *IEEE Commun. Lett.*, vol. 14, no. 10, pp. 900–902, 2010.

[25] A. Darwish and A. E. Hassanien, "Wearable and implantable wireless sensor network solutions for healthcare monitoring," *Sensors*, vol. 11, no. 6, pp. 5561–5595, 2011.

[26] S. Marinkovic and E. Popovici, "Network Coding for Efficient Error Recovery in Wireless Sensor Networks for Medical Applications," *2009 First Int. Conf. Emerg. Netw. Intell.*, pp. 15–20, 2009.

[27] R. R. Rout, S. Member, and S. K. Ghosh, "Enhancement of Lifetime using Duty Cycle and Network Coding in Wireless Sensor Networks," vol. 12, no. 2, pp. 656–667, 2013.

[28] K.-H. Lee, J.-H. Kim, and S. Cho, "Power saving mechanism with network coding in the bottleneck zone of multimedia sensor networks," *Comput. Networks*, vol. 96, pp. 58–68, 2016.

[29] A. Razzaque, C. S. Hong, and S. Lee, "Data-centric multiobjective QoS-aware routing protocol for body sensor networks," *Sensors*, vol. 11, no. 1, pp. 917–937, 2011.

[30] M. Monowar and M. M. Hassan, "Thermal-Aware Multiconstrained Intrabody QoS Routing for Wireless Body Area Networks," *... Sens. Networks*, vol. 2014, pp. 1–14, 2014.

[31] J. I. Bangash, A. W. Khan, and A. H. Abdullah, "Data-Centric Routing for Intra Wireless Body Sensor Networks," *J. Med. Syst.*, vol. 39, no. 9, 2015.

[32] B. Braem, B. Latré, I. Moerman, C. Blondia, E. Reusens, W. Joseph, L. Martens, and P. Demeester, "The need for cooperation and relaying in short-range high path loss sensor networks," *2007 Int. Conf. Sens. Technol. Appl. SENSORCOMM 2007, Proc.*, pp. 566–571, 2007.

[33] H. Alshaheen and H. Takruri Rizk, "Improving the energy efficiency for the WBSN bottleneck zone based on random linear network coding," *IET Wirel. Sens. Syst.*, pp. 1–9, 2017.

[34] M. K. Simon and M.-S. Alouini, *Digital communication over fading channels*, Edition, S. Canada: Hoboken, N.J.: Wiley-Interscience, 2005.

[35] Y. Suhov and M. Kelbert, *Probability and Statistics by Example*, vol. I. 2005.

[36] NIST is an agency of the U.S. Department of Commerce., "http://www.itl.nist.gov/div898/handbook/eda/section3/eda35g.htm," *NIST is an agency of the U.S. Department of Commerce.* .

[37] Vivax, "http://www.vivaxsolutions.com/maths/altrapzrule.aspx,"

[38] H. Alshaheen and H. Takruri Rizk, "Improving the Energy Efficiency for Biosensor Nodes in the WBSN Bottleneck Zone Based on a Random Linear Network Coding," in *IEEE Xplore,2017 11th International Symposium on Medical Information and Communication Technology (ISMICT)*, 2017, pp. 59–63.

[39] G. Grimmett and D. Stirzaker, *Probability and Random Processes*, Third. Great Britain: Oxford University Press Inc, 2001.

[40] W. W. Hines, D. C. Montgomery, D. M. Goldsman, and C. M. Borror, *Probability and Statistics in Engineering*, Fourth. USA: Argosy publishing, 2002.

2017 Vivax Solutions, 2017. .